ANTIMICROBIAL AGENTS AND CHEMOTHERAPY, July 2007, p. 2304–2312 Vol. 51, No. 7
0066-4804/07/$08.00+0 doi:10.1128/AAC.01438-06
Copyright © 2007, American Society for Microbiology. All Rights Reserved.

Transcriptional Response of *Candida parapsilosis* following Exposure to Farnesol▽†

Tristan Rossignol,[1]‡ Mary E. Logue,[1] Kieran Reynolds,[1] Muriel Grenon,[2] Noel F. Lowndes,[2] and Geraldine Butler[1]*

UCD School of Biomolecular and Biomedical Science, Conway Institute, University College Dublin, Belfield, Dublin 4, Ireland,[1] *and Genome Stability Laboratory, Department of Biochemistry and National Centre for Biomedical Engineering Science, National University of Ireland, Galway, Ireland*[2]

Received 17 November 2006/Returned for modification 9 January 2007/Accepted 28 April 2007

In *Candida albicans*, the quorum-sensing molecule farnesol inhibits the transition from yeast to hyphae but has no effect on cellular growth. We show that the addition of exogenous farnesol to cultures of *Candida parapsilosis* causes the cells to arrest, but not at a specific stage in the cell cycle. The cells are not susceptible to additional farnesol. However, the cells do eventually recover from arrest. Unlike in *C. albicans*, in *C. parapsilosis* sterols are localized to the tips of budding cells, and this polarization is disrupted by the addition of farnesol. We used the results of a genome sequence survey to design and manufacture partial genomic microarrays that were applied to determining the transcriptional response of *C. parapsilosis* to the presence of exogenous farnesol. In both *C. albicans* and *C. parapsilosis*, exposure to farnesol results in increased expression of the oxidoreductases *GRP2* and *ADH7* and altered expression of genes involved in sterol metabolism. There is no effect on expression of *C. parapsilosis* orthologs of genes involved in hyphal growth in *C. albicans*. Farnesol therefore differs significantly in its effects on *C. parapsilosis* and *C. albicans*.

Although *Candida albicans* is the most common cause of candidiasis, other species are becoming increasingly prevalent. *Candida parapsilosis* is now frequently reported as the most common non-*albicans* species in bloodstream infections in Europe (3, 38, 39), North America (14, 39), and Latin America (38, 39). Recent epidemiological studies ranked *C. parapsilosis* as the most prevalent yeast isolated from patients diagnosed with candidemia in a Japanese hospital in a 10-year period (39.2%) (33) and in a pediatric unit in Brazil (38.5%) (38). *C. parapsilosis* infections are predominantly associated with premature neonates, the presence of central venous catheters, and parenteral nutrition. *C. parapsilosis*, like other *Candida* species, can form biofilms on plastic medical devices, which confers resistance to antifungal drugs (4). Biofilm formation in *C. albicans* is associated with the switch from the yeast to the hyphal mode of growth (41). Unlike *C. albicans* strains, *C. parapsilosis* strains do not form true hyphae (36).

The formation of biofilms by *C. albicans* is inhibited by the addition of the isoprenoid alcohol farnesol (40). Farnesol is generated by dephosphorylation of farnesyl pyrophosphate, a key metabolic intermediate in the highly conserved sterol biosynthesis pathway in mammalian and yeast cells (11, 34, 47). In *C. albicans*, farnesol acts as a quorum-sensing agent (17). It inhibits the yeast-to-hypha transition without affecting the growth rate (17). However, the addition of exogenous farnesol inhibits growth in *Saccharomyces cerevisiae* (27) and triggers apoptosis in *Aspergillus nidulans* (45). Farnesol also reduces biofilm formation by *C. parapsilosis*, although because there is no link to hyphal growth, it is likely that the mechanism is different from that of *C. albicans* (25).

Until recently, little was known about the genome of *C. parapsilosis*. The complete mitochondrial genome was reported in 2004 (35), and we released the first sequence survey of the nuclear genome in 2005 (26). These genomic data allowed us to develop and manufacture oligonucleotide microarrays representing 3,849 putative open reading frames (ORFs) from *C. parapsilosis*. This provides for the first time a tool for analyzing the global pattern of gene expression of this species. We report here the impact of farnesol on the growth and gene expression of *C. parapsilosis* CLIB214.

MATERIALS AND METHODS

Strain and growth conditions. The type strain *C. parapsilosis* CLIB214 was used throughout this study. Fresh *trans*,*trans*-farnesol solution (Sigma) was prepared at a concentration of 40 mM in methanol, kept at 4°C, and used at the indicated final concentrations. The viability of the cells was calculated by counting CFU 1 h and 2 h following the addition of either methanol (control) or 50 μM farnesol. Viability was also assessed using staining with propidium iodide (PI). After 2 h of treatment with 50 μM farnesol, the cells were washed twice in phosphate-buffered saline (PBS), resuspended in PBS containing PI (Sigma) at 10 μg ml^{-1}, and incubated for 5 min. The cells were mounted on a microscope slide in the presence of Vectashield (Vector laboratories). The percentage of dead cells was determined by fluorescence microscopy using a Texas Red filter. At least 150 cells were counted in three independent experiments.

To determine the effect of farnesol on growth, *C. parapsilosis* CLIB214 was grown overnight in YPD medium (2% glucose, 2% Bacto peptone, 1% yeast extract) and diluted to an A_{600} of 0.2 in 50 ml of YPD at 30°C or 37°C supplemented with 10% (vol/vol) fetal calf serum (FCS) where indicated. Farnesol was added at the time point indicated at a final concentration of 10 μM, 50 μM, or 100 μM. Growth was monitored either by counting cells or by measuring A_{600}. Cell cycle experiments were performed as described in O'Shaughnessy et al. (37).

* Corresponding author. Mailing address: UCD School of Biomolecular and Biomedical Science, Conway Institute, University College Dublin, Belfield, Dublin 4, Ireland. Phone: 353-1-7166885. Fax: 353-1-2837211. E-mail: geraldine.butler@ucd.ie.

† Supplemental material for this article may be found at http://aac.asm.org/.

‡ Present address: Unité Biologie et Pathogénicité Fongiques, INRA USC 2019, Institut Pasteur, 25 Rue du Docteur Roux, 75724 Paris Cedex 15, France.

▽ Published ahead of print on 7 May 2007.

Cell cultures were counted using a Z2 coulter particle count and size analyzer (Beckman Coulter), and budding cells were counted under an Axioskop 2 plus (Zeiss) or an Olympus BX60 microscope.

For RNA isolation and for microscopy experiments, the strain was grown overnight in YPD medium at 30°C and diluted to an A_{600} of 0.2 in 50 ml of YPD at 30°C. Farnesol was added 4 h after the start of growth (corresponding to an A_{600} of 0.8) at a final concentration of 50 μM. Equal volumes of methanol were added to the control experiments. For microscopy, cells were collected after 1 h, and for RNA isolation, cells were collected after 2 h.

For biofilm experiments and crystal violet assays, the strain was grown overnight in YNB medium (0.67% yeast nitrogen base without amino acids, 0.75% amino acid dropout mixture, and 2% glucose) and diluted to an A_{600} of 1 in YNB medium. Cells were allowed to adhere in a Nunclon 96-well plate (Nunc) for 2 h at 37°C, and the wells were washed twice with PBS to remove nonadhered cells. One hundred microliters of fresh YNB was then added to the wells, and the plates were incubated for 24 h at 37°C.

Biofilm mass was determined with a crystal violet assay (9, 22, 42) as described in Laffey and Butler (25) with slight modifications. Briefly, biofilms formed in the 96-well plates were washed three times with 200 μl PBS, stained by adding 100 μl 0.1% aqueous crystal violet solution, and incubated at 30°C for 15 min. The plates were washed with sterile distilled water in an automatic plate washer (Tecan) and destained with 100 μl 33% (vol/vol) glacial acetic acid. After 4 h of destaining, 100 μl H_2O was added and 50 μl of this reaction mixture was transferred to a new 96-well plate. The amount of crystal violet stain in the destaining solution was measured spectrophotometrically at A_{570} (48).

Design of oligonucleotides for microarrays. Partial gene sequences for 3,954 putative ORFs were identified from a genome sequence survey of *C. parapsilosis* CLIB214 (26). For each ORF, a 68-base gene-specific oligonucleotide was designed using OligoArray 2.1 software (http://berry.engin.umich.edu/oligoarray2_1/). All probes were designed to have a midpoint temperature of 80°C ± 5°C in a first round of design (92% of the oligonucleotides) and a midpoint temperature of 80°C ± 10°C for the remaining probes, using OligoWiz 2 software (54). The presence of potential secondary structures was detected using the auxiliary program OligoArrayAux 2.1. Probes containing potential secondary structures were rejected and redesigned. The following criteria were also implemented in OligoArray2.1: a GC content between 20% and 50%, a maximum distance of 1,000 bp upstream of the potential 3′ end of the predicted gene sequence, and an absence of homopolymers. Potential cross-hybridizations were detected using OligoArray2.1. We also carried out our own homology-based approach for detection of cross-hybridization by using BLASTN and a series of dedicated PERL scripts. All designed oligonucleotides were compared to two separate databases: the entire set of *C. parapsilosis* contigs and reads generated by the genome assembly (from the genome sequence survey) and the *C. albicans* Assembly 19 haploid ORF set (23). If there was an unexpected match in either database with an alignment of at least 50 bp and an identity of at least 70% or a contiguous alignment of at least 24 bp with 100% identity, the oligonucleotide was considered nonspecific and redesigned. Oligonucleotides containing more than one base with a PHRED score of less than 15 from the genome sequence survey (26) were redesigned. For some ORFs, an oligonucleotide could not be designed to meet this cutoff, and the PHRED score cutoff was reduced to 10. The specificities of all oligonucleotides were later confirmed using the almost complete genome sequence data for *C. parapsilosis* obtained from the Sanger Institute (ftp://ftp.sanger.ac.uk/pub/pathogens/Candida/parapsilosis/C_parapsilosis.contigs.012406). Ninety-one percent of the designed oligonucleotides matched their intended targets with at least 99% identity, and the lowest identity score for the remaining oligonucleotides was 86%. In addition, two oligonucleotides were designed from rRNA sequences of *Escherichia coli* and *Arabidopsis thaliana* for use as positive controls.

Microarray production. Oligonucleotides were synthesized by Operon Biotechnologies and resuspended in printing buffer from Genetix at a final concentration of 50 μM. In total, 3,851 oligonucleotides, representing 3,849 putative genes and the two positive controls, were printed in duplicate on UltraGAPS coated slides (Corning), using a Q-array robot (Genetix) controlled with QSoft software (Genetix). The general design is two subarrays of 16 blocks each, with all oligonucleotides spotted in duplicate and one copy per block. The slides were air dried for 2 days, and DNA was cross-linked to the slide by UV at 6,200 mJ cm^{-2} in a UV linker (Stratagene). The slides were presoaked in a solution consisting of 75% PBS, 25% ethanol, and 0.5% sodium borohydride (Alfa Aesar) for 4 h at 42°C to remove potential spot autofluorescence. The slides were subsequently washed three times in water and one time in isopropanol, dried, and stored. Spot morphology and printing consistency were assessed for one slide in each batch by using SpotCheck solution (Genetix), following the manufacturer's instructions. Slides were considered to be of usable quality if at least 95% of the spots were present and unflagged by GenePix software (Axon Instruments).

TABLE 1. List of the primers used for RT-PCR experiments

Primer name	Sequence	Target
BUT33	ATGATAGAGTTGAAAGTAGTTTGGTCAATA	ACT1
BUT34	ACTACTGCTGAAAGAGAAATTGTTAGAGAC	ACT1
BUT47	CAAACAATTATGTCACCCAAGG	ADH7
BUT48	GTGAAGGACTAACCTCGAAC	ADH7
BUT136	CGTCAGAGACGTTGCAAAAG	GRP2
BUT137	TTGGAGCCTTTGATTCATCC	GRP2
BUT138	CGGAAAAACCTTGATGCAGT	ERG1
BUT139	ACAACAACATGGGGAATGGT	ERG1
BUT140	CCAGGTGTACCAAGCGAAAT	PCK1
BUT141	CCAGCTTCTTGAACCTCAGC	PCK1
BUT169	ATTGGCCAAGAGACACAAGG	GLN1
BUT170	GGTCAATGTTGGAAGCTGGT	GLN1
BUT175	CAGGTGGAGTTTTCGGTGTT	ERG6
BUT176	CCAACAGCTTCCGTGGTAAT	ERG6
BUT177	TGGAGTTTGAAGGGTTGTCC	ERG9
BUT178	CCGCACTTGATACCGATCTT	ERG9
BUT179	GTGATCGTGGAGAGGACCAT	PFK1
BUT180	TCCTCGTCCCCTTCTTCTTT	PFK1
BUT181	ATGGTGCATCAGCTCACTTG	FBP1
BUT182	CATGGGGAAACCTTCGTAAA	FBP1

Annotation of potential genes. Annotations were assigned to many of the putative *C. parapsilosis* ORF sequences by BLASTX comparison with *S. cerevisiae*, *C. albicans* (Assembly 19 haploid ORF set, April 2006), and the nonredundant-gene database from GenBank. The strongest BLASTX score was considered to be the ortholog, provided that the E value for this hit was less than 1e−10. Related annotations were obtained from SGD (http://www.yeastgenome.org/) for *S. cerevisiae*, from CGD (http://www.candidagenome.org/download/) and CandidaDB (ftp://ftp.pasteur.fr/pub/GenomeDB/CandidaDB/FlatFiles/) for *C. albicans*, and from GenBank (http://www.ncbi.nlm.nih.gov/).

RNA extraction. RNA was extracted from 50 ml of culture by using a RiboPure yeast kit (Ambion) according to the manufacturer's instructions. The concentration, quality, and integrity levels of the RNA samples were controlled using an Agilent 2100 bioanalyzer (Agilent) according to the manufacturer's instructions. Only samples with 28S/18S rRNA ratios between 1.6 and 2.2 and showing an absence of degradation were used in subsequent analysis.

RT-PCR. Reverse transcription (RT)-PCR was carried out as described previously (24) with the following modifications: the PCR regime used included a 1-min 30-s hot start at 95°C, followed by a 26-cycle program composed of a 40-s denaturation step at 95°C, a 2-min annealing step at 55°C, and a 3-min extension step at 72°C, followed by a 5-min final extension step at 72°C. The oligonucleotides used for RT-PCR were designed using Primer3 web-based software (http://fokker.wi.mit.edu/cgi-bin/primer3/primer3_www.cgi) and are listed in Table 1. Band intensities were visualized with GeneSnap software (Syngene, Cambridge, England) and quantified with GeneTools software (Syngene, Cambridge, England). The signal for each gene was normalized to the *ACT1* signal.

Transcriptional profiling. Twenty-five micrograms of total RNA was first incubated with 200 pmol of anchored oligonucleotide deoxyribosylthymine (Invitrogen) for 10 min at 70°C. First-strand buffer (1×; Invitrogen), 1.5 mM dATP, dTTP, and dGTP; 25 μM dCTP; 10 mM dithiothreitol; 2 μl Superscript II reverse transcriptase (Invitrogen); and 37.5 μM Cy3-dCTP or 37.5 μM Cy5-dCTP (Amersham) were added to a total volume of 40 μl. The mixture was incubated at 42°C for 2 h. An additional 1 μl of Superscript II was added to the mixture, and the incubation was continued for 1 h at 42°C. RNA was degraded by addition of 1 μl of RNase A (QIAGEN) at 50 μg ml^{-1} and 1 μl of RNase H (Invitrogen) at 0.05 unit μl^{-1} and incubated at 37°C for 30 min. The labeled cDNAs were purified using a QIAquick PCR purification kit (QIAGEN), following the manufacturer's instructions.

Microarray slides were prehybridized with in 5× SSC (1× SSC is 0.15 M NaCl plus 0.015 M sodium citrate), 0.1% sodium dodecyl sulfate (SDS), 10 mg ml^{-1} bovine serum albumin for 1 h at 42°C, washed three times in water and one time in isopropanol, and dried.

Incorporation of Cy3 and Cy5 dyes into cDNA targets was quantified by measuring the absorbance of each sample at 260 nm, 550 nm, or 650 nm. Samples were used if incorporation was greater than 15 pmol. The labeled cDNAs were concentrated by drying them under a vacuum, resuspended, and pooled in 45 μl of hybridization buffer (1× DigEasy [Roche] containing 0.5 mg ml^{-1} baker's yeast tRNA [Invitrogen] and 0.5 mg ml^{-1} salmon sperm DNA [Sigma]). The

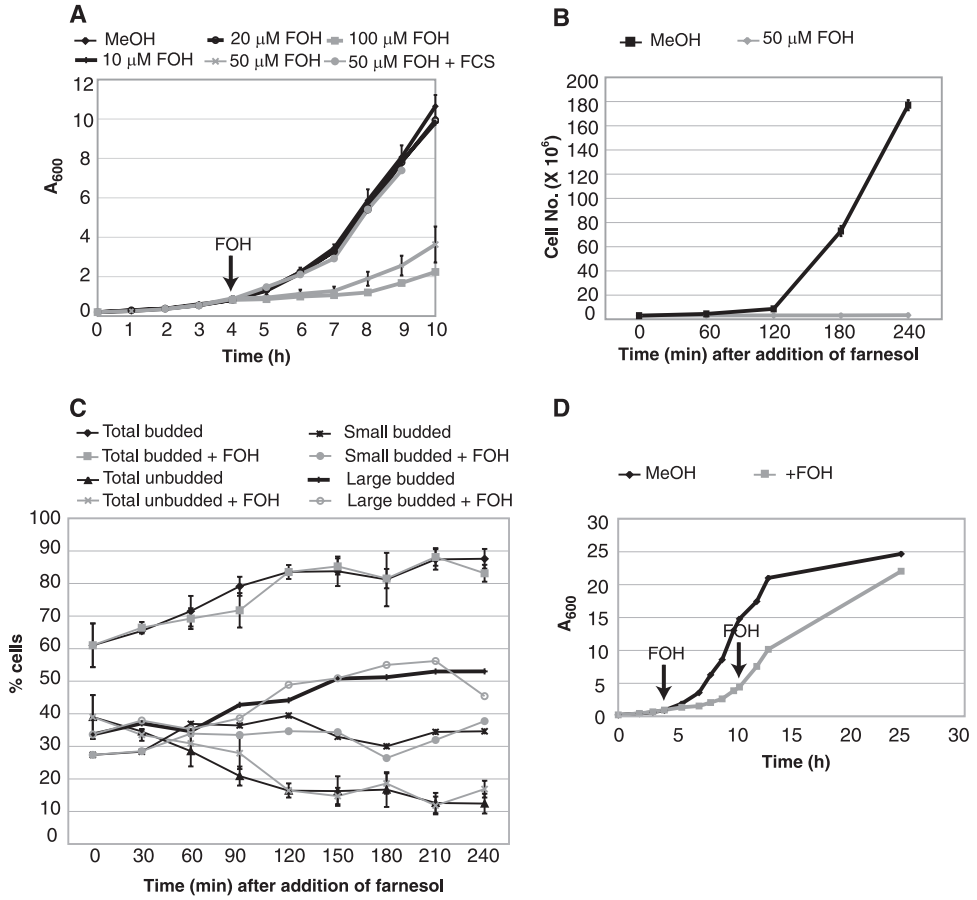

FIG. 1. Effect of farnesol on growth of *C. parapsilosis* CLIB214. (A) Cells were grown overnight in YPD at 30°C, diluted into fresh media, and allowed to grow for 4 h before the addition of farnesol at 10 μM, 20 μM, 50 μM, or 100 μM (indicated with an arrow). For one sample, 10% FCS was added at the same time as 50 μM farnesol. Growth was determined in three independent experiments by measuring absorbance at 600 nm, and the error bars show the standard deviations. Error bars were omitted from some data sets for clarity. (B) Cells were grown to exponential phase for 4 h before addition of methanol (MeOH) or 50 μM farnesol (time zero). Total cell number was determined by counting every 60 min. The averages for two samples from one experiment are shown. (C) Cells were grown to exponential phase for 4 h before addition of methanol (MeOH) or 50 μM farnesol (time zero). The percentages of cells with no buds (G_1), small buds (S), or large buds (G_2/M) were determined for samples taken every 30 min. The averages for two independent experiments are shown, and some error bars are omitted for clarity. (D) Cells were grown overnight in YPD at 30°C, diluted into fresh media, and allowed to grow for 4 h before the addition of farnesol at 50 μM where indicated. Farnesol (50 μM) was added for a second time after 10.5 h. Growth was determined by measuring absorbance at 600 nm. A representative example from two independent experiments is shown.

mixture was denatured at 95°C for 2 min, quickly cooled on ice, applied to the DNA microarray, and covered with a 24-mm by 60-mm coverslip. Slides were placed in a hybridization chamber (Corning, Palo Alto, CA) and incubated at 42°C for approximately 16 h. The slides were washed in 1× SSC at 42°C until the coverslip fell off and then washed three times for 10 min in 1× SSC, 0.1% SDS at 42°C and three times for 5 min in 1× SSC at 42°C and finally rinsed in 0.2× SSC at room temperature. The slides were dried by centrifugation at 1,000 rpm for 5 min. Six independent experiment comparisons (including three dye swaps) were performed.

The microarrays were scanned with an Axon 4000B scanner (Axon Instruments) at a 10-μm resolution. Data were acquired with GenePix Pro 5.0 software (Axon Instruments), and low-quality spots were automatically flagged. In addition, spots that were saturated or did not have background-corrected intensities greater than 20 in the Cy3 or the Cy5 channel were flagged. Normalization of the data was performed using the Lowess method in GeneSpring (Agilent Technologies). Spots present in at least three of the six slides were included in the subsequent analysis. The data set was statistically analyzed with SAM software (50) using the one-class response and performing 64 permutations. A false-discovery rate of 5.3% was selected to identify regulated genes, and genes with a <1.5-fold change in gene expression were removed.

Gene Ontology (GO) analyses were performed with GoToolBox web-based software (28), using *S. cerevisiae* gene GO term data for process and function analysis. We used the list of all the putative *C. parapsilosis* ORFs with *S. cerevisiae* orthologs annotated in GoToolBox as the reference gene set (representing 2,764 nonredundant genes). GO term analysis was also performed with *C. albicans* orthologs (3,784 annotated genes), using the GO term finder tool at the CGD website (http://www.candidagenome.org/).

Fluorescence microscopy. Cells were harvested, washed in 1× PBS, resuspended in water containing 100 μg ml^{-1} of filipin (Sigma), and incubated for 10 min at room temperature. The cells were mounted on glass slides for microscopic analysis using an Olympus BX60 microscope quipped with a 100-W mercury lamp and a narrow-band UV filter cube (excitation at 360 to 370 nm, with an emission filter at 420 to 460 nm). Images were captured using an F-View 2 digital camera (Soft Imaging Systems).

Microarray data accession number. The entire array data have been deposited in the NCBI Gene Expression Omnibus (GEO) (http://www.ncbi.nlm.nih.gov) and are accessible through GEO series accession number GSE6318.

RESULTS

Farnesol inhibits the growth of *C. parapsilosis*. We reported previously that the addition of farnesol reduces biofilm formation by three isolates of *C. parapsilosis* (25). We first confirmed

that farnesol has a similar effect on the type strain *C. parapsilosis* CLIB214. Biofilm formation is reduced up to 30% in the presence of 100 μM of farnesol for this strain (data not shown). The addition of exogenous farnesol also reduces biofilm development by *C. albicans* (6, 40). However, it is believed that this is caused by inhibiting the transition from yeast to hyphal growth, a phenomenon that does not occur in *C. parapsilosis* (33). We therefore tested whether farnesol inhibits growth of *C. parapsilosis*, as has been reported to occur in *S. cerevisiae* (27). Growth in liquid culture was monitored following the addition of 10 μM, 20 μM, 50 μM, and 100 μM of farnesol. Adding farnesol at 10 μM to 20 μM has no effect on growth, but adding 50 μM or 100 μM results in a strong inhibition (Fig. 1A). Counting cells showed that growth is dramatically inhibited within 2 h of the addition of farnesol (Fig. 1B). The observed arrest is not associated with any particular stage of the cell cycle, as the proportion of unbudded, small budded, or large budded cells, indicative of cells in G_1, S, or G_2/M phase, respectively, does not vary in the farnesol-treated and untreated-population (Fig. 1C). This was confirmed by fluorescence-activated cell sorting analysis (not shown). It is therefore likely that farnesol treatment has no effect on cell cycle progression. The total inhibition of growth is specific to farnesol and is not seen, for example, when Triton X-100 or SDS is added at similar concentrations (data not shown). This suggests that farnesol is not simply acting like a detergent.

The addition of 50 μM farnesol induces death in up to 20% of the cells after 2 h (determined by measuring survival with colony counts and by staining with PI). The methanol-treated control population has 90 to 95% viability. The difference in viability, however, is not sufficient to account for the total inhibition of growth observed.

Growth is delayed for at least 4 h before cells reenter the exponential phase. The delay is longer in the presence of 100 μM farnesol than with 50 μM (Fig. 1A). The cells do recover from the growth delay, and after 24 h, the cell densities are almost equivalent between the treated and nontreated cultures. Growth is not further inhibited if farnesol is added a second time (at 10.5 h) (Fig. 1D), and it is therefore unlikely that the recovery is due to the loss or evaporation of farnesol. However, if the cells are diluted following overnight growth, they are once again sensitive to farnesol (not shown). The growth arrest was also confirmed using different media (YPD, synthetic defined, and RPMI) and at different temperatures (30°C and 37°C). The strong repression and the delay in restarting growth were observed in all cases, with some variation in the length of the delay (data not shown). We did not, however, observe any change in morphology or size in the cells following the addition of farnesol, using either microscopy or a cell size analyzer.

Mosel et al. (31) have suggested that farnesol is bound or sequestered by serum. We therefore determined the effect of simultaneously adding both serum and farnesol to the medium. In the presence of 10% FCS, the inhibitory effect of farnesol is totally alleviated at both 30°C (Fig. 1A) and 37°C (not shown).

In the experiments whose results are shown in Fig. 1, farnesol was added after 4 h of growth in a fresh medium. We also tested the effect of adding farnesol at different time points (Table 2). A maximum inhibition of growth (up to 88.5%) is obtained following an addition of farnesol after 4 h (A_{600} at 0.8). The inhibition of growth is lower when farnesol is added at 6 h (A_{600} at 2.3) and is very weak when farnesol is added after 8 h of growth (A_{600} at 6). Addition of farnesol at 2 h also results in inhibition of growth up to 71%. As the addition after 4 h is the most effective, this time point was used in the transcriptional profiling experiments.

TABLE 2. Growth inhibition following addition of farnesol at different times

Time of addition (h)[a]	% Inhibition[b] after indicated time	
	2 h	4 h
0	NA	25.5 ± 11.5
2	68.5 ± 9.5	71 ± 9
4	88.5 ± 4.5	83 ± 1
6	40.5 ± 3.5	49 ± 5
8	9.5 ± 4.5	16 ± 2

[a] Cells from an overnight culture were inoculated into fresh media, grown for the time indicated, and farnesol was added at a final concentration of 50 μM.

[b] Percent inhibition of growth 2 h or 4 h after the addition of farnesol was calculated using the following formula: percent inhibition = $[1 - (\Delta_{farnesol}/\Delta_{ref})] \times 100$, where Δ is the difference between the absorbance value at 2 h or 4 h after addition of farnesol and that at the time of addition, $\Delta_{farnesol}$ is the value for the farnesol treatment set, and Δ_{ref} is the value for the reference set. Absorbance was measured at 600 nm. These results are based on two replicates. NA, not available.

Transcriptional profiling. To identify genes that are differentially regulated in *C. parapsilosis* following exposure to farnesol, we performed transcriptional profiling experiments using partial genomic microarrays. From the 3,954 putative ORF sequences identified from the genome sequence survey of *C. parapsilosis* (26) (covering roughly 0.8 of the haploid genome), we were able to design and print gene-specific oligonucleotides for 3,849 putative ORFs, using the criteria described in Materials and Methods. A total of 3,784 ORFs have identifiable orthologs in *C. albicans* (BLAST E value, <1e−10), corresponding to approximately 60% of the nonoverlapping ORFs predicted in the haploid *C. albicans* genome, and 3,003 have identifiable *S. cerevisiae* orthologs (BLAST E value, <1e-10).

The gene expression analysis was first performed following exposure to both 10 μM and 50 μM of farnesol. We observed few changes in gene expressions with 10 μM of farnesol (data not shown), which is in agreement with the absence of a growth inhibition effect that we observed at this concentration. We therefore focused on the effect of adding 50 μM farnesol. Expression was analyzed 2 h after the addition of farnesol, chosen to maximize the differences directly caused by farnesol. After statistical analysis of six individual comparisons, we identified 312 genes with increased expression and 280 genes with reduced expression in farnesol-treated cells. All data are available in Table S1 in the supplemental material.

The addition of farnesol has the most dramatic effect on expression of *GRP2* (expression increased 15-fold) and *ADH7* (expression increased 6-fold) (see Table S1 in the supplemental material). Two closely related genes, *ADH1* and *GRE3*, also show increased expression. These are all categorized as oxidoreductases, and 24 genes in this functional category have increased expression upon exposure to farnesol (not shown). The increased expressions of *GRP2* and *ADH7* were confirmed by RT-PCR (Fig. 2A).

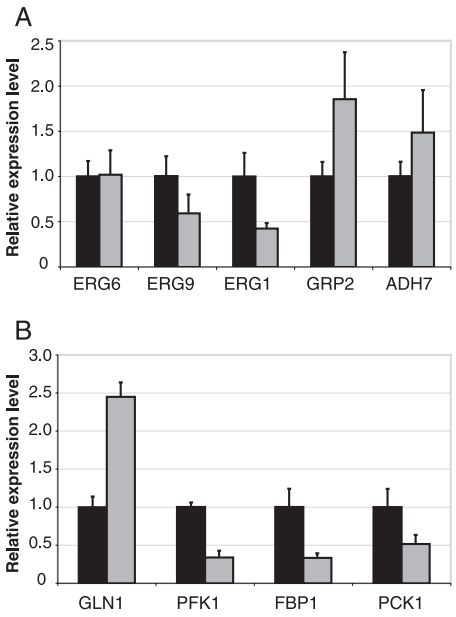

FIG. 2. RT-PCR analysis of nine genes identified as differentially expressed by microarray experiments. The signal for each gene was normalized to the *ACT1* signal for each sample, and the expression level of the untreated sample was set to 1 for each gene. The values are averages for five independent RNA preparations, and error bars indicate standard deviations. Black bars represent the control experiment; gray bars represent the addition of farnesol. (A) Genes involved in ergosterol metabolism and genes coding for oxidoreductases. (B) Genes involved in glutamate metabolism and hexose metabolism. All genes show the same effect on expression as with the microarrays, except *ERG6*, for which differential expression was not seen with RT-PCR.

GO analysis. As no GO terms are currently assigned to *C. parapsilosis* and few are assigned to *C. albicans*, we identified *S. cerevisiae* orthologs and used the associated GO terms. Among the regulated genes, 244 of those with increased expression and 196 of those with decreased expression had *S. cerevisiae* orthologs annotated in GoToolBox, representing 78% and 70% of the total, respectively. GO terms assigned to both process and function analyses were used, and the process analyses provided more significant results. The full list of GO terms, associated genes, and statistical significance is available in Table S2 in the supplemental material. A similar analysis using the *C. albicans* GO annotation generated equivalent results, except that the cellular lipid metabolism category was not represented in genes with reduced expression (data not shown).

Table 3 shows a selection of the most relevant process GO terms (with a *P* value of <0.05) that are overrepresented or underrepresented in the genes with altered expression, and some of the categories are described below.

Lipid metabolism genes. The addition of farnesol has a major effect on genes involved in lipid metabolism. Twenty-one genes, including 2 genes with the same *S. cerevisiae* ortholog, *LRO1* (acyl transferase), have increased expression, whereas 15 have reduced expression (Table 3). Several are directly linked to ergosterol biosynthesis, six with increased expression (*ERG6*, *ERG7*, *ERG4*, *NCP1*, *MCR1*, and *MVD1*) and three with reduced expression (*ERG1*, *ERG25*, and

TABLE 3. Selected process GO terms overrepresented following exposure to farnesol

Data set and term[a]	Value for genes in indicated group				*P*
	Reference[b]		Farnesol treatment[c]		
	No.	Frequency	No.	Frequency	
Up-regulated genes					
Ribosome biogenesis	138	0.0510	23	0.0943	0.001295
Steroid metabolism	30	0.0111	8	0.0328	0.003047
Glutamate metabolism	14	0.0052	5	0.0205	0.004986
rRNA processing	111	0.0410	18	0.0738	0.005025
Ergosterol metabolism	20	0.0074	6	0.0246	0.005392
Cellular lipid metabolism	132	0.0488	20	0.082	0.006628
rRNA metabolism	115	0.0425	18	0.0738	0.006963
RNA metabolism	275	0.1016	35	0.1434	0.007517
Sterol metabolism	28	0.0103	7	0.0287	0.007638
tRNA metabolism	72	0.0266	12	0.0492	0.014608
Glutamine family amino acid biosynthesis	21	0.0078	5	0.0265	0.026417
Serine family amino acid metabolism	15	0.0055	4	0.0164	0.03165
Down-regulated genes					
Alcohol metabolism	94	0.0347	15	0.0765	0.001659
Hexose metabolism	44	0.0163	8	0.0408	0.008564
GPI anchor metabolism	13	0.0048	4	0.0204	0.009842
Gluconeogenesis	17	0.0063	4	0.0204	0.024365
Cellular lipid metabolism	132	0.0488	15	0.0765	0.024601

[a] The list of processes was simplified to remove overlapping categories and categories with ≤3 genes or ≥500 genes.
[b] Number or frequency of genes in each category in the reference set (total, 2,764 genes).
[c] Number or frequency of farnesol-enriched genes in each category in the up-regulated-gene (total, 244 genes) and down-regulated-gene (total, 196 genes) data sets. The complete list is available in Table S2 in the supplemental material.

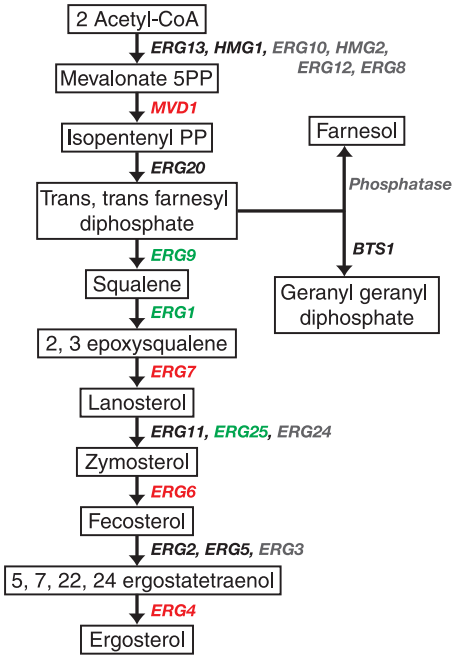

FIG. 3. Simplified ergosterol metabolism pathway as described for *S. cerevisiae* (http://www.yeastgenome.org/). Genes indicated in red are up-regulated in *C. parapsilosis* following addition of farnesol, genes indicated in green are down-regulated by farnesol addition, genes indicated in black show no reproducible change in expression, and genes indicated in gray are absent from our arrays.

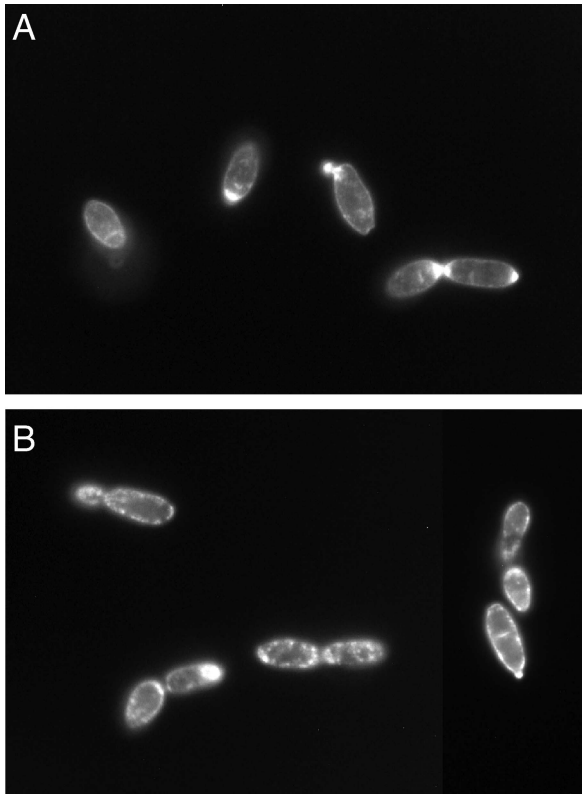

FIG. 4. Localization of membrane sterols in *C. parapsilosis*. Shown are representative images of cells stained with filipin in the control experiment without addition (A) and 1 h after addition of farnesol at 50 μM (B).

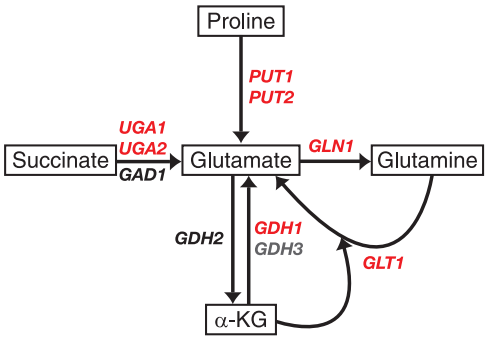

FIG. 5. Glutamate metabolism pathway as described for *S. cerevisiae* (http://www.yeastgenome.org/). Genes indicated in red are up-regulated in *C. parapsilosis* following addition of farnesol, the expressions of genes indicated in black are not reproducibly altered, and genes indicated in gray are not present on our arrays.

ERG9). In *S. cerevisiae*, farnesol is synthesized from *trans*,*trans*-farnesyl diphosphate as part of the ergosterol pathway (Fig. 3). The three genes in *C. parapsilosis* with reduced expression are active just after the branch leading to farnesol (Fig. 3). The reductions in *ERG1* and *ERG9* expression were confirmed by RT-PCR (Fig. 2A). The addition of exogenous farnesol appears to have a general effect on the ergosterol pathway, as 50% of the genes involved in the ergosterol pathway present on our arrays are differentially expressed.

The changes in the expressions of sterol synthesis genes prompted us to determine the effect of farnesol on the localization of sterols by using filipin staining. In the absence of farnesol, 49% ($n = 121$) of the cells harbored staining at the growing bud tip (Fig. 4A) and 51% had uniform staining throughout the cell. Only 18% ($n = 151$) of cells treated with farnesol harbored strong tip staining, whereas 82% were stained uniformly or randomly (Fig. 4B). This suggests that sterol distribution is perturbed in the presence of farnesol.

The transcriptional profiling experiments also show that genes involved in other lipid pathways are differentially expressed in response to farnesol. Several genes from the phospholipid metabolism have decreased expression, including four required for glycosylphosphatidylinositol (GPI) anchor biosynthesis (Table 3).

Genes involved in ribosome biogenesis. The most significantly overrepresented category among genes with increased expression following exposure to farnesol is ribosome biogenesis, which includes 23 genes (Table 3). This represents 9.5% of the genes with increased expression. Ribosome biogenesis is among the most statistically underrepresented terms for genes with decreased expression, with only four genes in this category (see Table S2 in the supplemental material). These results suggest that translation may be higher in cells exposed to farnesol than in the control.

Amino acid and hexose metabolism genes. Exposure to farnesol results in increases in the expressions of several genes involved in amino acid metabolism (Table 3), including those for serine family amino acid metabolism (*CYS4*, *YNL247W*, *HOM6*, and *GCV1*). Most notably, we see overrepresentation of homologs of genes involved in glutamate and glutamine metabolism in *S. cerevisiae* (Fig. 5), including *PUT2*, *GLT1*, *PUT1*, *GDH1*, *UGA2*, and *GLN1* and two ORFs which match the same *S. cerevisiae* ortholog, *UGA1*. Of the 10 putative orthologs in *C. parapsilosis*, 7 are up-regulated in response to farnesol, 1 (*GDH3*) is not present in our array, and only 2 (*GDH2* and *GAD1*) have unchanged expression. Overexpression of *GLN1* in response to farnesol was confirmed by RT-PCR (Fig. 2B).

In contrast, the addition of farnesol results in reduced expression for eight genes involved in hexose metabolism (Table 3): *PCK1*, *FBP1*, *PFK1*, *PFK26*, *CAT8*, *GID8*, *GAL10*, and *GAL7*. The down-regulation of *PCK1*, *FBP1*, and *PFK1* was confirmed by RT-PCR (Fig. 3B). These genes are mostly involved in the upper part of the glucose metabolism pathway (both gluconeogenesis and glycolysis) and in particular the conversion of fructose-6-phosphate into fructose-1,6-biphosphate (*PFK1*, *PFK26*, and *FBP1*). Genes involved in the lower part of the pathway from fructose-1,6-biphosphate to pyruvate represented in our arrays do not have altered expression.

DISCUSSION

In this study, we describe the effect of adding exogenous farnesol on *C. parapsilosis* at the physiological and transcriptional levels. We show that addition of farnesol causes growth arrest of *C. parapsilosis* in liquid culture. The arrest is alleviated when farnesol is bound to serum proteins, suggesting that it is directly affecting the cells.

One significant difference between the growth inhibitions

observed in *C. parapsilosis* and *S. cerevisiae* is that farnesol does not induce arrest at a specific stage in the cell cycle in *C. parapsilosis*, whereas *S. cerevisiae* shows an increase in unbudded cells following the addition of farnesol (27). Another difference is that the *C. parapsilosis* cells eventually recover, and by 24 h, the cell densities are approximately the same in cells treated and not treated with farnesol. Adding more farnesol at later times does not increase the lag in growth (Fig. 1D), although if the cells are diluted into fresh culture following overnight growth, they recover sensitivity to farnesol. It is therefore likely that sensitivity to farnesol is restricted to early stages in growth or to low population densities.

The addition of farnesol induces apoptosis in *Candida dubliniensis*, *A. nidulans*, and mammalian cells and kills up to 80% of *C. albicans* opaque-phase cells (10, 20, 30, 44, 45, 52). Approximately 20% of *C. parapsilosis* cells die following 2 h of exposure to 50 μM farnesol. This may be associated with the expression of five genes (*SNF1*, *GTS1*, *SCH9*, *ATP2*, and *LAG1*) involved in cell aging (21), and this category is significantly overrepresented in the up-regulated genes (see Table S2 in the supplemental material).

Two groups have recently reported the transcriptional response of *C. albicans* to the presence of exogenous farnesol (6, 12). We found little correlation with the work of Cao et al. (6), who measured changes in expression 24 h after treatment with farnesol. There are significant similarities, and substantial differences, between our results with *C. parapsilosis* and those for the *C. albicans* experiments described by Enjalbert and Whiteway (12). The expressions of orthologs of *ADH7* (a member of the NADPH-dependent cinnamyl alcohol dehydrogenase family) and *GRP2* (related to the *GRE2* family of NADPH-dependent methyglyoxal reductases) show the greatest increases in response to farnesol in *C. parapsilosis* (see Table S1 in the supplemental material). Expression of *ADH7* (*orf19.5517*) is highly induced in the presence of farnesol in *C. albicans* (12). *GRP2* is also induced, but at a lower level. Warringer and Blomberg (53) showed that *S. cerevisiae gre2*Δ strains have increased sensitivity to inhibitors of the ergosterol pathway, and those authors suggest that Gre2p is involved in detoxification of intermediate accumulation. It is therefore likely that oxidoreductases play a major role in responding to farnesol in both species, possibly acting through the ergosterol pathway.

It is not surprising that the addition of farnesol affects the expression of genes involved in ergosterol metabolism, as farnesol is synthesized as part of this pathway. Inhibition of the pathway by the addition of several azoles increases the production of farnesol in *C. albicans* up to 45-fold (18, 19). The perturbation of sterol synthesis might also explain the effect of farnesol on other components of the lipid pathway, as crosstalk between ergosterol and fatty acid pathways in *S. cerevisiae*, for example, has already been shown (51).

As our results suggest that farnesol affects sterol synthesis at the transcriptional level in *C. parapsilosis*, we used filipin staining to determine if there are changes in sterol localization. Filipin is a polyene that binds sterols and is often used to determine the positions of lipid rafts (29). Martin and Konopka (29) showed that in *C. albicans*, filipin stains sterols at the tips of hyphae, but there is no polarization in budding or pseudohyphal cells. Polarization, however, is not affected by the addition of farnesol. In contrast, our results show that in *C. parapsilosis*, there is obvious polarization of sterols to the tips of budding cells, and to bud necks, in cells at different stages of the cell cycle (Fig. 5A). The addition of farnesol disrupts this polarization in the majority of cells. This suggests that farnesol may affect membrane structure in *C. parapsilosis* and therefore may affect membrane permeability. Changes in the membrane permeability of *C. dubliniensis* in response to farnesol treatment have also been reported (20). Lipid rafts are associated with specific proteins, such as Pma1p in *S. cerevisiae* (49) and GPI-anchored proteins in *S. cerevisiae* (1) and mammalian cells (5). Interestingly, we have shown that several genes involved in GPI anchor biosynthesis have decreased expression in *C. parapsilosis* following exposure to farnesol, correlating with the changes in the localization of the lipid raft.

In *C. albicans*, farnesol acts as a quorum-sensing agent, and one of the most obvious effects is that it represses the expression of hypha-specific genes (12). We did not detect any effect of farnesol on the expression of orthologs of these genes in *C. parapsilosis*, which correlates with the observation that *C. parapsilosis* cannot generate true hyphae (15). We therefore do not know if farnesol is used as a quorum-sensing molecule in *C. parapsilosis*. There is one report that media conditioned by the growth of *C. parapsilosis* cannot inhibit filamentation by *C. albicans*, whereas media conditioned with *Candida tropicalis* or *C. dubliniensis* can (15). We also cannot detect any inhibition caused by *C. parapsilosis*-conditioned media (not shown). This suggests that farnesol is not produced by *C. parapsilosis.* However, the *C. parapsilosis* genome appears to possess all the genes required for synthesis, including the final step, recently shown to be catalyzed by the *DPP3* gene (34). *A. nidulans* also apparently does not produce farnesol, yet exogenous addition induces apoptosis (45). It is possible, therefore, that *C. parapsilosis* simply responds to the presence of quorum-sensing agents secreted by other fungi or bacteria, which may be used to control growth or simply to communicate between species (13, 16). For example, mixed infection with both *C. parapsilosis* and *C. albicans* has been reported (43). It is also likely that other quorum-sensing molecules remain to be identified, such as tyrosol identified in *C. albicans* (8) and aromatic alcohols identified in *S. cerevisiae* (7).

The increases in the expressions of genes involved in ribosome biogenesis in *C. parapsilosis* following exposure to farnesol are surprising, as we have shown that growth is inhibited. However, similar increases are observed in *C. albicans* within 10 min of treatment (12) (see the supplemental material), which may reflect the synthesis of proteins specifically needed for the response to the farnesol signal.

We observed increases in the expressions of glutamate metabolism genes in *C. parapsilosis* (Fig. 5), which are also induced in *S. cerevisiae* during stationary growth following depletion of carbon and nitrogen sources (46). The increased expressions of these genes in *C. parapsilosis*, and the decreased expressions of genes involved in hexose and amino acid metabolism, may be correlated with growth arrest.

In conclusion, we have shown that despite some similarities between the responses of *C. albicans* and *C. parapsilosis* to the addition of exogenous farnesol, there are also substantial differences. Addition of farnesol inhibits growth in *C. parapsilosis* and has no effect on morphology. In *C. albicans*, growth is not inhibited and the morphological transition to hyphae is greatly

reduced. However, biofilm formation is inhibited in both yeasts (25, 40). It has generally been assumed that the effect of farnesol on biofilm development by *C. albicans* is related to the inhibition of hyphal growth, as hyphae are required for biofilms in this species (2, 41). Our results suggest that the inhibition of biofilms may be due to common effects of farnesol in the two species, such as increases in the expressions of the oxidoreductase genes *ADH7* and *GRP2*. Metabolism of alcohol has been associated with biofilm development in *C. albicans*, and disruption of the *CaADH1* gene significantly enhances the ability to form biofilms (32). It will be interesting to determine if a similar mechanism operates in *C. parapsilosis.*

To our knowledge, this is the first study using microarrays to analyze changes in gene expression in *C. parapsilosis*. Our arrays were designed on the basis of a genome sequence survey, but an almost complete genome sequence of isolate *C. parapsilosis CDC317* has been carried out by the Wellcome Trust Sanger Institute and is now available (http://www.sanger.ac.uk/sequencing/Candida/parapsilosis/). This will allow us to manufacture whole-genome arrays. We have shown that results from *C. albicans* cannot simply be assumed to be also true of *C. parapsilosis*, and a better understanding of the biology of the latter organism is needed at the physiological and genomic level.

ACKNOWLEDGMENTS

This study was supported by Science Foundation Ireland and the Health Research Board.

REFERENCES

1. **Bagnat, M., and K. Simons.** 2002. Cell surface polarization during yeast mating. Proc. Natl. Acad. Sci. USA **99:**14183–14188.
2. **Baillie, G. S., and L. J. Douglas.** 1999. Role of dimorphism in the development of *Candida albicans* biofilms. J. Med. Microbiol. **48:**671–679.
3. **Bedini, A., C. Venturelli, C. Mussini, G. Guaraldi, M. Codeluppi, V. Borghi, F. Rumpianesi, F. Barchiesi, and R. Esposito.** 2006. Epidemiology of candidaemia and antifungal susceptibility patterns in an Italian tertiary-care hospital. Clin. Microbiol. Infect. **12:**75–80.
4. **Branchini, M. L., M. A. Pfaller, J. Rhine-Chalberg, T. Frempong, and H. D. Isenberg.** 1994. Genotypic variation and slime production among blood and catheter isolates of *Candida parapsilosis*. J. Clin. Microbiol. **32:**452–456.
5. **Brown, D. A., and E. London.** 1998. Functions of lipid rafts in biological membranes. Annu. Rev. Cell Dev. Biol. **14:**111–136.
6. **Cao, Y.-Y., Y.-B. Cao, Z. Xu, K. Ying, Y. Li, Y. Xie, Z.-Y. Zhu, W.-S. Chen, and Y.-Y. Jiang.** 2005. cDNA microarray analysis of differential gene expression in *Candida albicans* biofilms exposed to farnesol. Antimicrob. Agents Chemother. **49:**584–589.
7. **Chen, H., and G. R. Fink.** 2006. Feedback control of morphogenesis in fungi by aromatic alcohols. Genes Dev. **20:**1150–1161.
8. **Chen, H., M. Fujita, Q. Feng, J. Clardy, and G. R. Fink.** 2004. Tyrosol is a quorum-sensing molecule in *Candida albicans*. Proc. Natl. Acad. Sci. USA **101:**5048–5052.
9. **Djordjevic, D., M. Wiedmann, and L. A. McLandsborough.** 2002. Microtiter plate assay for assessment of *Listeria monocytogene*s biofilm formation. Appl. Environ. Microbiol. **68:**2950–2958.
10. **Dumitru, R., D. H. Navarathna, C. P. Semighini, C. G. Elowsky, R. V. Dumitru, D. Dignard, M. Whiteway, A. L. Atkin, and K. W. Nickerson.** 2007. In vivo and in vitro anaerobic mating in *Candida albicans*. Eukaryot. Cell **6:**465–472.
11. **Edwards, P. A., and J. Ericsson.** 1999. Sterols and isoprenoids: signaling molecules derived from the cholesterol biosynthetic pathway. Annu. Rev. Biochem. **68:**157–185.
12. **Enjalbert, B., and M. Whiteway.** 2005. Release from quorum-sensing molecules triggers hyphal formation during *Candida albicans* resumption of growth. Eukaryot. Cell **4:**1203–1210.
13. **Federle, M. J., and B. L. Bassler.** 2003. Interspecies communication in bacteria. J. Clin. Investig. **112:**1291–1299.
14. **Fridkin, S. K., D. Kaufman, J. R. Edwards, S. Shetty, and T. Horan.** 2006. Changing incidence of *Candida* bloodstream infections among NICU patients in the United States: 1995–2004. Pediatrics **117:**1680–1687.
15. **Hazen, K. C., and J. E. Cutler.** 1979. Autoregulation of germ tube formation by *Candida albicans*. Infect. Immun. **24:**661–666.
16. **Hogan, D. A.** 2006. Talking to themselves: autoregulation and quorum sensing in fungi. Eukaryot. Cell **5:**613–619.
17. **Hornby, J. M., E. C. Jensen, A. D. Lisec, J. J. Tasto, B. Jahnke, R. Shoemaker, P. Dussault, and K. W. Nickerson.** 2001. Quorum sensing in the dimorphic fungus *Candida albicans* is mediated by farnesol. Appl. Environ. Microbiol. **67:**2982–2992.
18. **Hornby, J. M., B. W. Kebaara, and K. W. Nickerson.** 2003. Farnesol biosynthesis in *Candida albicans*: cellular response to sterol inhibition by zaragozic acid B. Antimicrob. Agents Chemother. **47:**2366–2369.
19. **Hornby, J. M., and K. W. Nickerson.** 2004. Enhanced production of farnesol by *Candida albicans* treated with four azoles. Antimicrob. Agents Chemother. **48:**2305–2307.
20. **Jabra-Rizk, M. A., M. Shirtliff, C. James, and T. Meiller.** 2006. Effect of farnesol on *Candida dubliniensis* biofilm formation and fluconazole resistance. FEMS Yeast Res. **6:**1063–1073.
21. **Jazwinski, S. M.** 2002. Growing old: metabolic control and yeast aging. Annu. Rev. Microbiol. **56:**769–792.
22. **Jin, Y., H. K. Yip, Y. H. Samaranayake, J. Y. Yau, and L. P. Samaranayake.** 2003. Biofilm-forming ability of *Candida albicans* is unlikely to contribute to high levels of oral yeast carriage in cases of human immunodeficiency virus infection. J. Clin. Microbiol. **41:**2961–2967.
23. **Jones, T., N. A. Federspiel, H. Chibana, J. Dungan, S. Kalman, B. B. Magee, G. Newport, Y. R. Thorstenson, N. Agabian, P. T. Magee, R. W. Davis, and S. Scherer.** 2004. The diploid genome sequence of *Candida albicans*. Proc. Natl. Acad. Sci. USA **101:**7329–7334.
24. **Kelly, M. T., D. M. MacCallum, S. D. Clancy, F. C. Odds, A. J. P. Brown, and G. Butler.** 2004. The *Candida albicans CaACE2* gene affects morphogenesis, adherence and virulence. Mol. Microbiol. **53:**969–983.
25. **Laffey, S. F., and G. Butler.** 2005. Phenotype switching affects biofilm formation by *Candida parapsilosis*. Microbiology **151:**1073–1081.
26. **Logue, M. E., S. Wong, K. H. Wolfe, and G. Butler.** 2005. A genome sequence survey shows that the pathogenic yeast *Candida parapsilosis* has a defective *MTLa1* allele at its mating type locus. Eukaryot. Cell **4:**1009–1017.
27. **Machida, K., T. Tanaka, Y. Yano, S. Otani, and M. Taniguchi.** 1999. Farnesol-induced growth inhibition in *Saccharomyces cerevisiae* by a cell cycle mechanism. Microbiology **145:**293–299.
28. **Martin, D., C. Brun, E. Remy, P. Mouren, D. Thieffry, and B. Jacq.** 2004. GOToolBox: functional analysis of gene datasets based on Gene Ontology. Genome Biol. **5:**R101.
29. **Martin, S. W., and J. B. Konopka.** 2004. Lipid raft polarization contributes to hyphal growth in *Candida albicans*. Eukaryot. Cell **3:**675–684.
30. **Miquel, K., A. Pradines, and G. Favre.** 1996. Farnesol and geranylgeraniol induce actin cytoskeleton disorganization and apoptosis in A549 lung adenocarcinoma cells. Biochem. Biophys. Res. Commun. **225:**869–876.
31. **Mosel, D. D., R. Dumitru, J. M. Hornby, A. L. Atkin, and K. W. Nickerson.** 2005. Farnesol concentrations required to block germ tube formation in *Candida albicans* in the presence and absence of serum. Appl. Environ. Microbiol. **71:**4938–4940.
32. **Mukherjee, P. K., S. Mohamed, J. Chandra, D. Kuhn, S. Liu, O. S. Antar, R. Munyon, A. P. Mitchell, D. Andes, M. R. Chance, M. Rouabhia, and M. A. Ghannoum.** 2006. Alcohol dehydrogenase restricts the ability of the pathogen *Candida albicans* to form a biofilm on catheter surfaces through an ethanol-based mechanism. Infect. Immun. **74:**3804–3816.
33. **Nakamura, T., and H. Takahashi.** 2006. Epidemiological study of *Candida* infections in blood: susceptibilities of *Candida* spp. to antifungal agents, and clinical features associated with the candidemia. J. Infect. Chemother. **12:**132–138.
34. **Navarathna, D. H., J. M. Hornby, N. Krishnan, A. Parkhurst, G. E. Duhamel, and K. W. Nickerson.** 2007. Effect of farnesol on a mouse model of systemic candidiasis, determined by use of a *DPP3* knockout mutant of *Candida albicans*. Infect. Immun. **75:**1609–1618.
35. **Nosek, J., M. Novotna, Z. Hlavatovicova, D. W. Ussery, J. Fajkus, and L. Tomaska.** 2004. Complete DNA sequence of the linear mitochondrial genome of the pathogenic yeast *Candida parapsilosis*. Mol. Genet. Genomics **272:**173–180.
36. **Odds, F. C.** 1988. Candida and candidosis: a review and bibliography. Bailliere and Tindall, London, United Kingdom.
37. **O'Shaughnessy, A. M., M. Grenon, C. Gilbert, G. W. Toh, C. M. Green, and N. F. Lowndes.** 2006. Multiple approaches to study *S. cerevisiae* Rad9, a prototypical checkpoint protein. Methods Enzymol. **409:**131–150.
38. **Pasqualotto, A. C., W. L. Nedel, T. S. Machado, and L. C. Severo.** 2005. A 9-year study comparing risk factors and the outcome of paediatric and adults with nosocomial candidaemia. Mycopathologia **160:**111–116.
39. **Pfaller, M. A., D. J. Diekema, R. N. Jones, H. S. Sader, A. C. Fluit, R. J. Hollis, S. A. Messer, and SENTRY Participant Group.** 2001. International surveillance of bloodstream infections due to *Candida* species: frequency of occurrence and in vitro susceptibilities to fluconazole, ravuconazole, and voriconazole of isolates collected from 1997 through 1999 in the SENTRY Antimicrobial Surveillance Program. J. Clin. Microbiol. **39:**3254–3259.
40. **Ramage, G., S. P. Saville, B. L. Wickes, and J. L. Lopez-Ribot.** 2002. Inhibition of *Candida albicans* biofilm formation by farnesol, a quorum-sensing molecule. Appl. Environ. Microbiol. **68:**5459–5463.

41. **Ramage, G., K. VandeWalle, J. L. Lopez-Ribot, and B. L. Wickes.** 2002. The filamentation pathway controlled by the Efg1 regulator protein is required for normal biofilm formation and development in *Candida albicans*. FEMS Microbiol. Lett. **214:**95–100.
42. **Reynolds, T. B., and G. R. Fink.** 2001. Bakers' yeast, a model for fungal biofilm formation. Science **291:**878–881.
43. **Richter, S. S., R. P. Galask, S. A. Messer, R. J. Hollis, D. J. Diekema, and M. A. Pfaller.** 2005. Antifungal susceptibilities of *Candida* species causing vuvovaginitis and epidemiology of recurrent cases. J. Clin. Microbiol. **43:** 2155–2162.
44. **Rioja, A., A. R. Pizzey, C. M. Marson, and N. S. B. Thomas.** 2000. Preferential induction of apoptosis of leukaemic cells by farnesol. FEBS Lett. **467:**291–295.
45. **Semighini, C. P., J. M. Hornby, R. Dumitru, K. W. Nickerson, and S. D. Harris.** 2006. Farnesol-induced apoptosis in *Aspergillus nidulans* reveals a possible mechanism for antagonistic interactions between fungi. Mol. Microbiol. **59:**753–764.
46. **Shamji, A. F., F. G. Kuruvilla, and S. L. Schreiber.** 2000. Partitioning the transcriptional program induced by rapamycin among the effectors of the Tor proteins. Curr. Biol. **10:**1574–1581.
47. **Song, L.** 2006. A soluble form of phosphatase in *Saccharomyces cerevisiae* capable of converting farnesyl diphosphate into E,E-farnesol. Appl. Biochem. Biotechnol. **128:**149–158.
48. **Stepanovic, S., D. Vukovic, I. Dakic, B. Savic, and M. Svabic-Vlahovic.** 2000. A modified microtiter-plate test for quantification of staphylococcal biofilm formation. J. Microbiol. Methods **40:**175–179.
49. **Toulmay, A., and R. Schneiter.** 2007. Lipid-dependent surface transport of the proton pumping ATPase: a model to study plasma membrane biogenesis in yeast. Biochimie **89:**249–254.
50. **Tusher, V. G., R. Tibshirani, and G. Chu.** 2001. Significance analysis of microarrays applied to the ionizing radiation response. Proc. Natl. Acad. Sci. USA **98:**5116–5121.
51. **Veen, M., and C. Lang.** 2005. Interactions of the ergosterol biosynthetic pathway with other lipid pathways. Biochem. Soc. Trans. **33:**1178–1181.
52. **Voziyan, P. A., J. S. Haug, and G. Melnykovych.** 1995. Mechanism of farnesol cytotoxicity: further evidence for the role of PKC-dependent signal transduction in farnesol-induced apoptotic cell death. Biochem. Biophys. Res. Commun. **212:**479–486.
53. **Warringer, J., and A. Blomberg.** 2006. Involvement of yeast Y*OL151W*/*GRE2* in ergosterol metabolism. Yeast **23:**389–398.
54. **Wernersson, R., and H. B. Nielsen.** 2005. OligoWiz 2.0–integrating sequence feature annotation into the design of microarray probes. Nucleic Acids Res. **33:**W611–W615.